Article

Not peer-reviewed version

Holothurian Wall Hydrolysates Ameliorate Cyclophosphamide-Induced Immunocompromised Mice via Regulating Immune Response and Improving Gut Microbiota

Chen Yan , Huiru Qu , Xinli Li * , Bin Feng

Posted Date: 13 July 2023

doi: 10.20944/preprints202307.0923.v1

Keywords: holothurian wall hydrolysates; immunodeficiency; tight junction proteins; pro-inflammatory cytokines; microbial composition

Article

Holothurian Wall Hydrolysates Ameliorate Cyclophosphamide-Induced Immunocompromised Mice via Regulating Immune Response and Improving Gut Microbiota

Chen Yan, Huiru Qu, Xinli Li * and Bin Feng *

Department of Biotechnology, College of Basic Medical Sciences, Dalian Medical University, Dalian 116044, China

* Correspondence: lixinlibio@hotmail.com (X.L.); Tel.: +86-411-8611-0296; binfeng@dmu.edu.cn (B.F); Tel.: +86-411-8611-8844

Abstract: Some biologically active compounds isolated from sea cucumbers stimulate the body's immune response through activating immune cells. Immune function is closed related to the integrity intestinal barrier and balanced gut microbiota. However, it is unknown whether daily administration of holothurian wall hydrolysates (HWH) ameliorated intestinal dysbiosis and barrier injury induced by immunodeficiency. This study aimed to investigate the immunomodulatory effect and the underlying mechanism of HWH in cyclophosphamide (CTX)-induced immunocompromised mice. BALB/c mice received CTX (80 mg/kg, intraperitoneally) once a day for 3 days to induce immunodeficiency, and then oral administration of HWH (80 or 240 mg/kg), levamisole hydrochloride (LH, 40 mg/kg, positive control) respectively once a day for 7 days. We utilized 16S rRNA sequencing for microbial composition alterations, histopathological analysis for splenic and colonic morphology, Western blotting for expressions of tight junction proteins (TJs), and quantitative real-time (qRT-PCR) for measurements of pro-inflammatory cytokines. HWH attenuated the immune organ damage induced by CTX, increased the secretions of interleukin (IL)-6, IL-1β and tumor necrosis factor (TNF)-α, and promoted the recovery of goblet cells and the productions of TJs (claudin-1, occludin, and ZO-1) in the colon of the immunocompromised mice. Moreover, HWH promoted the growth of beneficial microorganisms such as *Lactobacillus*, *Lachnospiraceae*, *Christensenellaceae*, and *Bifidobacterium*, while suppressed the populations of *Ruminococcus*, *Staphylococcus*, and *Streptococcus*. These results demonstrate that HWH elicits intestinal mucosal immunity, repairs the damage to intestinal mucosal integrity, and normalizes the imbalanced intestinal microbial profiles in immunocompromised mice. It may be helpful to identify the biological activities of HWH, and supports the potential as new prebiotics, immunomodulatory agents, and medical additive for intestinal repair.

Keywords: holothurian wall hydrolysates; immunodeficiency; tight junction proteins; pro-inflammatory cytokines; microbial composition

1. Introduction

The gastrointestinal (GI) tract of human is colonized by a huge number of microorganisms, termed gut microbiota [1]. Healthy gut microbiota contains *Bacteroidetes* and *Firmicutes* [2], followed by *Actinobacteria*, *Proteobacteria*, and *Verrucomicrobia* [3], as well as methanogenic archaea, eukaryote, and various phages [4]. Multiple host-endogenous and host-exogenous factors exert effects on the gut microbiota to make a resilient, stable and balanced microflora [5]. Individuals contain unique intestine flora that distinguish them from the population. They can be identified uniquely among populations of 100s based on the microbiomes using metagenomic codes [6].

 doi:10.20944/preprints202307.0923.v1

Once there are alterations in those influencing factors, such as genetic mutations, dietary preference, and antibiotics administration, the dysbiosis of gut microbiota occurs. The dysbiosis can induce the dysfunction of intestinal barrier, the influx of pro-inflammatory bacterial fragments, and low-grade chronic systemic inflammation [7]. Various studies have shown the associations between dysbacteriosis and obesity [8], type 2 diabetes [9], hypertension [10], and inflammatory bowel disease [11].

The gut microbiota can prevent exogenous infections through antimicrobial agents production, nutrient competition, intestinal barrier integrity improvement, bacteriophage utilization, and immune response activation [12]. Besides, gut microbiota also occupy binding sites in the mucus layer covering enterocytes, and prevent pathogens from colonizing the intestine of human [13]. Intestinal epithelial barrier and immune system contribute to gut barrier integrity, thereby preventing risk factors, and maintaining a symbiotic relation with other bacteria [14, 15]. The intestinal epithelial barrier contains several types of intestine epithelial cells (IEC). IECs form a strong barrier by adherens junctions, tight junctions, and desmosomes, which preventing the leakage of intracellular components and influx of exogenous pathogens through the intracellular space. The lamina propria of epithelial layer promotes healthy communication between gut microbiota and immune cells [15]. Moreover, intestinal immune cells (e.g., dendritic cells, T cells, B cells, and macrophages) are related with the IECs closely to remain intestinal homeostasis [16, 17].

There is a crucial relationship between the compromised immune function and the integrity intestinal barrier. Compromised immune function leads to impaired intestinal mucus barrier and disturbed gut microbiota [18, 19]. Recently immunomodulators for impaired immune function is developed to mainly stimulate impaired immunity, not to repair intestinal mucosal damage, and not to improve the health of gut microbiota. For example, (E)-phenethyl 3-(3,5-dihydroxy-4-isopropylphenyl) acrylate gels exerted its immunotherapeutic effects by modulating the balance of Th1/Th2/Th17/Treg cell subsets in allergic contact hypersensitivity [20]. Tiepishihu Xiyangshen granules has prominent immunomodulatory activities by regulating TLR4/MAPKs and PI3K/AKT/FOXO3a signal pathways [21]. However, gut microbiota and intestinal barrier act important roles in the chronic human diseases, it should not be ignored [22]. Therefore, the works focusing on effective methods to improve intestinal barrier function and repair the gut microbiota dysbiosis for immunodeficiency treatment are of great importance.

There is a long history of treating and preventing disease with natural products. Natural products especially from terrestrial creatures, have long been a traditional source of therapeutic components [23]. Many researchers consider marine invertebrates more fruitful sources of novel therapeutic agents than any group of terrestrial species, and marine compounds have gradually attracted attentions in recent years because of their unique structural and biological activities with less side effects [24, 25]. Sea cucumbers (class Holothuroidea), belonging to the phylum Echinodermata, are precious seafood and important sources of medicine. The main active ingredients contained polysaccharides, peptides, triterpene glycosides, etc., which have several important functions in the body, such as ameliorating glucose intolerance, inhibiting the growth of tumor, regulating the gut microbiota, and stimulating immunity [26-31]. Moreover, the latest study showed that *Holothuria leucospilota* polysaccharides played a role in treating constipation by optimizing intestinal flora composition, promoting intestinal peristalsis, relieving intestinal inflammation, and regulating intestinal electrolyte metabolism [32]. As a marine natural compound, sodium oligomannate (GV-971) therapeutically remodeled gut microbiota and suppressed gut bacterial amino acids-shaped neuroinflammation to inhibit Alzheimer's disease [33]. Our previous work [34] also indicated that chitosan against ulcerative colitis in mice through mitigating intestinal microflora dysbiosis, and regulating the expressions of TNF-α, claudin-1, occludin, and ZO-1. There is a potential mechanistic link between gut microbiota dysbiosis, intestinal barrier function and diseases.

In recent years, the active substances from sea cucumbers were shown to be effective inductors of the cellular immunity. However, there are few reports on the role of hydrolysates from sea cucumber in intestinal immunity, the underlying mechanism between holothurian wall hydrolysates (HWH) and the immune system remains unclear. Therefore, in the present study, a CTX-induced

Preprints (www.preprints.org) | NOT PEER-REVIEWED | Posted: 13 July 2023 doi:10.20944/preprints202307.0923.v1

immunocompromised mouse model was established to evaluate the immunomodulatory effect and the underlying mechanism of HWH treatment. The bacterial composition altered after CTX administration and HWH treatment by 16S rRNA sequencing. Furthermore, histopathological analysis was performed followed by TJs (claudin-1, occludin and ZO-1) and pro-inflammatory cytokines (TNF-α, IL-6, and IL-1β) analysis. Our focus were to investigate the impact of CTX on the intestinal barrier integrity and gut microbiota, and probe the potential of HWH as immunomodulator in the amelioration of intestinal dysbiosis, and restoration of intestinal barrier impairment in immunodeficiency, and provide a novel insight for enhancing the value of the sea cucumber.

2. Results

2.1. Peptide sequence analysis of HWH

The total protein content, total carbohydrate content, moisture content, and ash content of HWH were 91.93±0.42%, 0.76±0.05%, 2.60±0.05%, and 2.03±0.06%, respectively. LC-MS was used to obtain the total ion flow diagram of HWH (Figure 1). The peptide sequence identification result of HWH is shown in Table 1. The peptides detected in HWH were input to PeptideRanker for activity evaluation. A total of 23 peptides were identified in HWH, thereinto, the activity score of five peptides (AAVAAAVAPPSPPPIAGPP, FDGPEGPRGPPGSE, GFDGPEGPRGPPGSE, RGPAGPTGPTGPA, and SRGLLSCLF) were > 0.5. The peptides with high activity in HWH in molecular weight were 1649.91, 1397.62, 1454.64, 1134.57 and 1051.55 Da, respectively, and were mainly composed of peptides with 9-19 amino acids. These results showed that peptides were the main components of HWH.

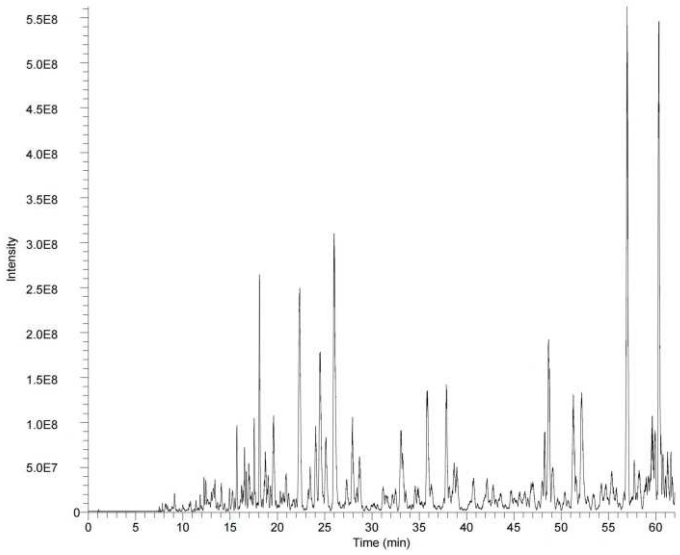

Figure 1. Total ion current diagram of HWH. Scanning range: 300-1400 *m*/*z*.

Table 1. Determination of the HWH peptide sequence by LC-MS.

Number	Sequence	Mass	Charges	Intensity	Activity Prediction Score
1	AAVAAAVAPPSPPPIAGPP	1649.91	2	179750	0.55
2	ALAALQQSSSSGSSSSTAT	1739.82	2	454080	0.19
3	ATKYSDITKLSSIGKSVE	1926.03	2	5239900	0.09
4	DLSEEFMAICSTMPDT	1845.75	2	2482400	0.42
5	DVITIEVLAK	1099.64	2	2187900	0.08
6	EKLCYVALDFEQEMATAASSSSLEK	2806.30	3	335090	0.04
7	FDGPEGPRGPPGSE	1397.62	2	4477600	0.55
8	FSGSQPELPVDQ	1302.61	2	8266800	0.26
9	GEAGAETPKAATEAGEAP	1655.76	2	4324000	0.14

Preprints (www.preprints.org) | NOT PEER-REVIEWED | Posted: 13 July 2023 doi:10.20944/preprints202307.0923.v1

10	GFDGPEGPRGPPGSE	1454.64	2	4834900	0.62
11	GIVLDSGDGVTH	1168.57	2	1385600	0.18
12	KGADGETGEPGPQG	1298.57	2	273750	0.22
13	LCYVALDFEQEMATAASSSSLEK	2549.17	3	23738000	0.03
14	LDLAGRDLTDY	1250.61	2	650410	0.16
15	LLSEMRRLE	1145.62	2	192180	0.22
16	MEHDTRTHREHYR	1766.80	2	13898000	0.06
17	PVSASRHQESANQGL	1579.77	2	6068000	0.20
18	RGPAGPTGPTGPA	1134.57	2	2150400	0.56
19	SPGEKGDQGSPGPA	1282.58	2	1278600	0.38
20	SRGLLSCLF	1051.55	2	371770	0.83
21	SYELPDGQVITIGNER	1789.88	2	765850	0.21
22	VAPEEHPVLLTEAPLNPK	1953.06	2	158170	0.34
23	YAYSVKNAVQDAP	1424.69	2	302260	0.09

2.2. Effects of HWH on spleen index and spleen histopathology

Histopathological images of spleens were shown in Figure 2A. In the NC and N240 groups, the red pulp and white pulp were clearly distinguished. The section of spleen in CTX group showed an unclear border between red pulp and white pulp, and abnormal tissue morphology. However, the boundary region between white pulp and red pulp in spleen was more apparent in HWH80 and HWH240 groups. Additionally, the HWH240 group demonstrated smaller spleen damage than that of HWH80 group due to clearer boundary between red pulp and white pulp, which was closer to the NC group. In addition, compared with the CTX group, the reduced damage in HWH80 and HWH240 groups reflected that HWH could alleviate CTX induced injury in spleen.

As shown in Figure 2B, the spleen indices of the CTX group were significantly decreased compared to those of the NC group. Compared to the CTX group, HWH80, HWH240, and PC groups showed a drastic increase in the spleen indices ($p < 0.001$), whereas there was no significant difference in the spleen indices of mice between the NC and N240 groups. HWH treatment effectively increased the spleen indices ($p < 0.05$), which implied HWH could reverse the CTX-induced immune dysfunction of spleen.

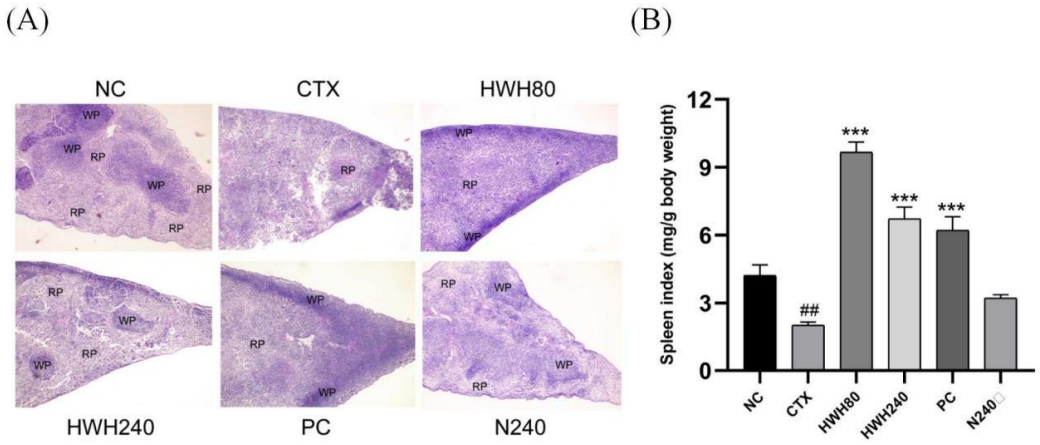

Figure 2. Effects of HWH on spleen histopathology and spleen indices in CTX-induced immunocompromised mice. Histopathology (magnification 40×) (A). Spleen indices (B). WP, white pulp; RP, red pulp. NC: Normal control mice; CTX: Mice treated with 80 mg/kg CTX alone; HWH80: Mice treated with CTX plus HWH (80 mg/kg); HWH240: Mice treated with CTX plus HWH (240 mg/kg); PC: Mice treated with CTX plus levamisole hydrochloride (40 mg/kg); N240: Mice treated with HWH (240 mg/kg). Values are shown as mean ± SD (n = 10). $^{\#\#}$ $p<0.01$ compared to NC; *** $p<0.001$ compared to CTX.

2.3. Effects of HWH on histopathology in colon

Preprints (www.preprints.org) | NOT PEER-REVIEWED | Posted: 13 July 2023 doi:10.20944/preprints202307.0923.v1

The histological analysis of colonic tissues was done by H&E staining (Figure 3A). NC group demonstrated a normal histology consisting of well-shaped and compact crypt containing goblet cells. In contrast, CTX-treated mice showed histological alterations consisting of blunt and short crypt with an obvious infiltration of inflammatory cells. However, HWH80, HWH240, and PC groups exhibited a reduced infiltration of inflammatory cells, and improved colonic tissue structure which was more similar to the NC group. N240 group also showed a normal and regular colonic wall structure lined with dark-stained nuclei in lamina propria.

PAS-positive goblet cells were observed in the crypts of colon (Figure 3A). The OD of CTX group was significantly lower than that of NC group ($p < 0.05$), whereas the OD of HWH80, HWH240, and PC groups was higher than that of CTX group significantly ($p<0.05$) (Figure 3B). In addition, there was no significant difference between the NC and N240 groups. The results indicated that HWH could repair the CTX-induced damage in the colon.

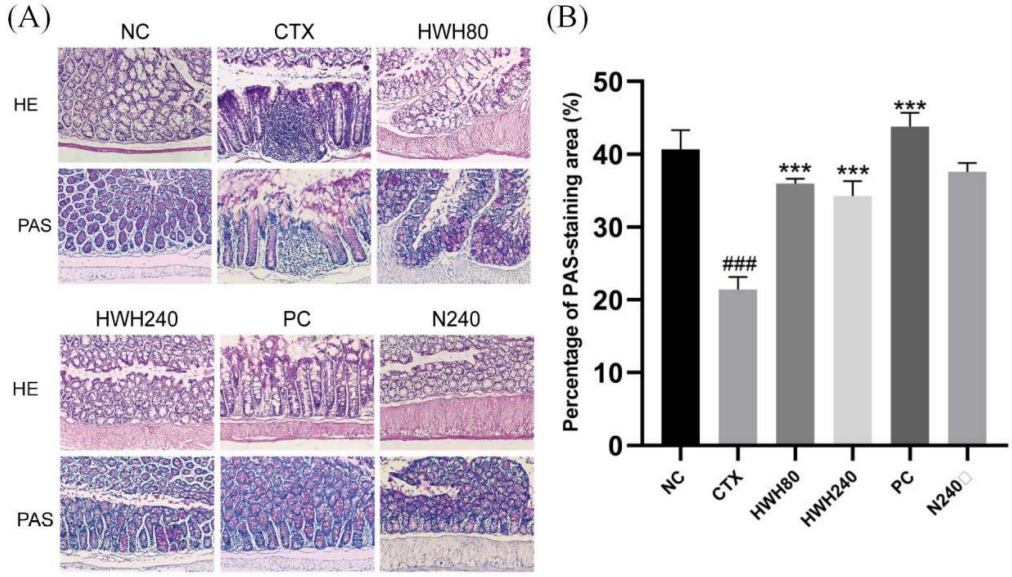

Figure 3. Effects of HWH on colon histopathology in CTX-induced immunocompromised mice. Representation of colon stained with H&E and PAS (magnification 100×) (A). Percentage of PAS-staining area (%) (B). NC: Normal control mice; CTX: Mice treated with 80 mg/kg CTX alone; HWH80: Mice treated with CTX plus HWH (80 mg/kg); HWH240: Mice treated with CTX plus HWH (240 mg/kg); PC: Mice treated with CTX plus levamisole hydrochloride (40 mg/kg); N240: Mice treated with HWH (240 mg/kg). Values are shown as mean ± SD (n = 10). *** $p < 0.001$ compared to CTX group, and $^{###}$ $p < 0.001$ compared to NC group.

2.4. Effects of HWH on intestinal tight junction proteins

Compared to the NC group, reduced expression of TJs was observed in the CTX group (Figure 4). HWH intervention enhanced the expression of TJs significantly in the HWH80 and HWH240 groups compared with the CTX group ($p<0.05$), whereas there was no significant difference between the NC and N240 group. These findings suggested that HWH could improve the expressions of TJs, and reduce the damage in the colon caused by CTX-induced immunodeficiency.

Preprints (www.preprints.org) | NOT PEER-REVIEWED | Posted: 13 July 2023 doi:10.20944/preprints202307.0923.v1

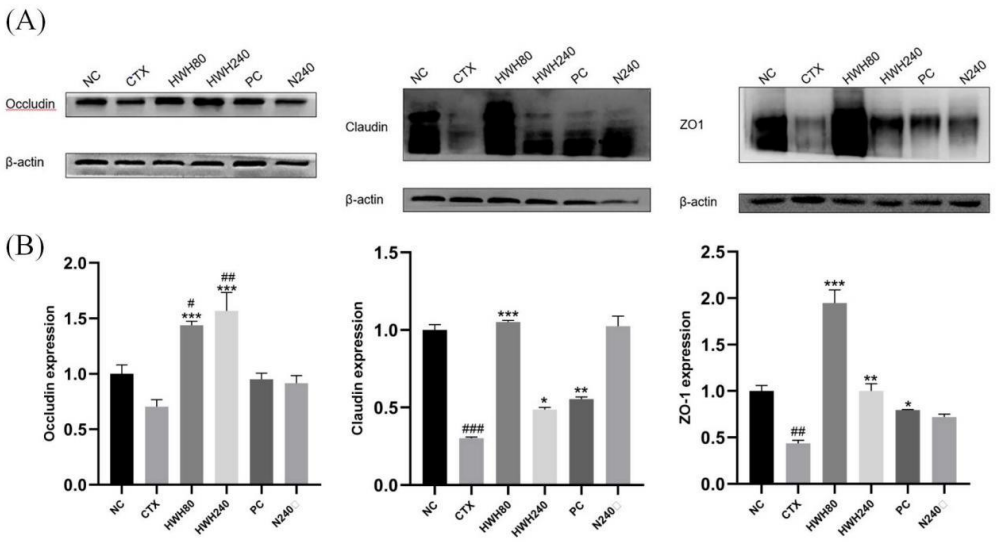

Figure 4. Effects of HWH on protein expressions of occludin, claudin, and ZO-1 in colon. NC: Normal control mice; CTX: Mice treated with 80 mg/kg CTX alone; HWH80: Mice treated with CTX plus HWH (80 mg/kg); HWH240: Mice treated with CTX plus HWH (240 mg/kg); PC: Mice treated with CTX plus levamisole hydrochloride (40 mg/kg); N240: Mice treated with HWH (240 mg/kg). Values are shown as mean ± SD (n = 10). $^{\#}$ $p < 0.05$, $^{\#\#}$ $p < 0.01$ and $^{\#\#\#}$ $p < 0.001$ compared with NC group; * $p < 0.05$, ** $p < 0.01$, and *** $p < 0.001$ compared with CTX group.

2.5. Effects of HWH on pro-inflammatory cytokines levels

Compared to the NC group, CTX reduced the levels of inflammatory cytokines (Figure 5). The HWH80, HWH240, and PC groups showed a significant increase compared to the CTX group in the levels of IL-6 and IL-1β ($p<0.05$), whereas merely HWH240 group showed a significant increase compared with CTX group in the level of TNF-α. Compared to the NC group, the significant increase of the N240 group indicated that HWH could improve the secretion of TNF-α. CTX induced a significant decrease of secretion of IL-6, implying the inhibitory effects of CTX on IL-6. These findings reflected that HWH reversed the CTX-induced decreased secretion of pro-inflammatory cytokines.

In addition, the HWH80, HWH240, and PC groups showed higher secretion of IL-1β compared to NC group significantly, while HWH240 demonstrated a significant increase in the secretion of IL-6, which indicated that HWH could increase the secretions of IL-1β and IL-6 in normal mice. The results reflected that HWH also promoted the secretion of immune cytokines.

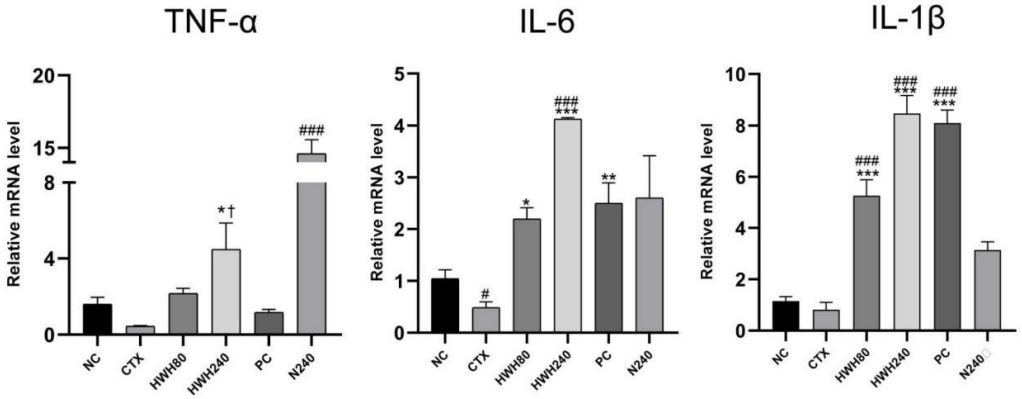

Figure 5. Effects of HWH on the mRNA levels of pro-inflammatory cytokines (IL-6, IL-1β, and TNF-α) in colon. NC: Normal control mice; CTX: Mice treated with 80 mg/kg CTX alone; HWH80: Mice treated with CTX plus HWH (80 mg/kg); HWH240: Mice treated with CTX plus HWH (240 mg/kg); PC: Mice treated with CTX plus levamisole hydrochloride (40 mg/kg); N240: Mice treated with HWH

Preprints (www.preprints.org) | NOT PEER-REVIEWED | Posted: 13 July 2023 doi:10.20944/preprints202307.0923.v1

(240 mg/kg). Values are shown as mean ± SD (n = 10). $^{\#}$ $p < 0.05$ and $^{\#\#\#}$ $p < 0.001$ compared to NC; * $p < 0.05$, ** $p < 0.01$ and *** $p < 0.001$ compared to the CTX group; † $p < 0.05$ compared to N240 group.

2.6. Effects of HWH on the overall composition of gut microbiota

16S rRNA gene sequencing was used to detect the gut microbial composition. Illumina pair-end sequencing returned 3,790,530 raw sequences across 18 fecal samples to investigate the dynamic alterations of the microbial composition in the gut. After paired-end reads assemblies and quality filtering, a total of 1,859,229 sequences were used in downstream analysis. The Rank abundance curve shown in Figure 6A, suggesting that the current sequencing depth has already found most of the microbial phylotypes. The richness and diversity in all the six groups were also observed by rank abundance, which showed high species richness and evenness in HWH-treated groups in general. Clustering at 97% identity produced 147,549 unique operational taxonomic units (OTUs) in total and 81,697 OTUs on average for each sample (ranging from 57,439 to 105,717), providing over 99.9% coverage of all samples. The details of sequences of all samples were shown in Table S2. A box-plot was plotted to indicate that higher α-diversity in HWH-H and N240 groups (Figure 6B). The results of Chao1, ACE, and OTU in HWH-treated groups were higher than that in CTX group (M) (Table S3), indicating diversity of species which was decreased due to CTX. These results concluded that CTX obviously reduced the overall microbial population in the gut. HWH treatment helped to restore the community of gut microbiota in partial.

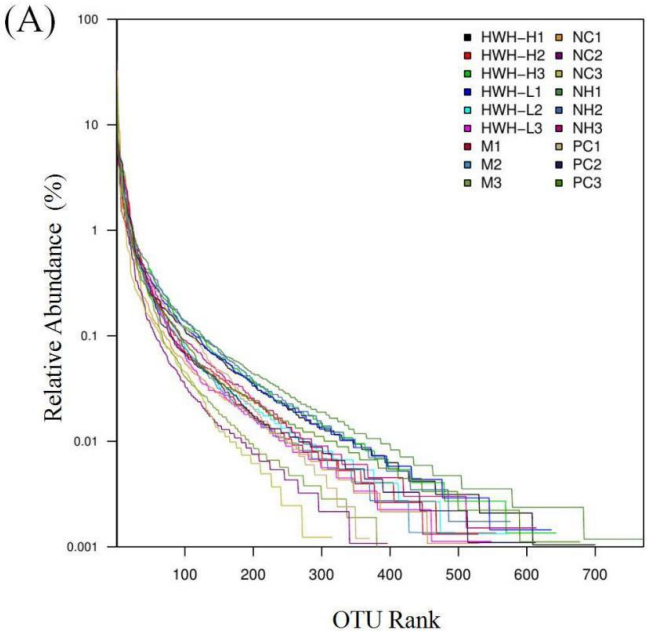

Preprints (www.preprints.org) | NOT PEER-REVIEWED | Posted: 13 July 2023 doi:10.20944/preprints202307.0923.v1

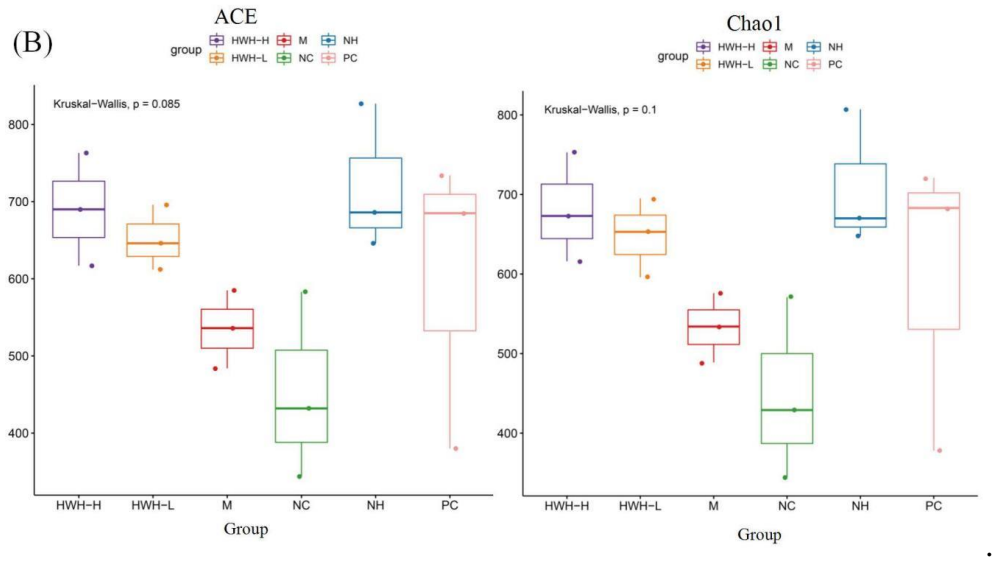

Figure 6. Effects of HWH on alpha diversity in CTX-induced immunocompromised mice. Rank abundance curve (A). Box plot of the gut microbiota (B). NC: Normal control mice; M: Mice treated with 80 mg/kg CTX alone (CTX); HWH-L: Mice treated with CTX plus HWH (80 mg/kg) (HWH80); HWH-H: Mice treated with CTX plus HWH (240 mg/kg) (HWH240); PC: Mice treated with CTX plus levamisole hydrochloride (40 mg/kg); NH: Mice treated with HWH (240 mg/kg) (N240).

2.7. Effects of HWH on beta diversity of gut microbiota

The beta diversity was determined by principal component analysis (PCA) and principal coordinate analysis (PCoA), which revealed bacterial community structural variation in all groups (Figure 7). The top two principal components in PCA analysis occupied 14.95% and 52.52% of variation of the overall data. It showed that the structure of microbial community in CTX group (M) was significantly different from that of NC group. PCoA analysis demonstrated that the microbial community structure in CTX group (M) was clustered distantly from NC group, and HWH-H group showed a much higher difference with CTX group than that of HWH-L group. PC group showed close to HWH-H group. These data were consistent with the α-diversity.

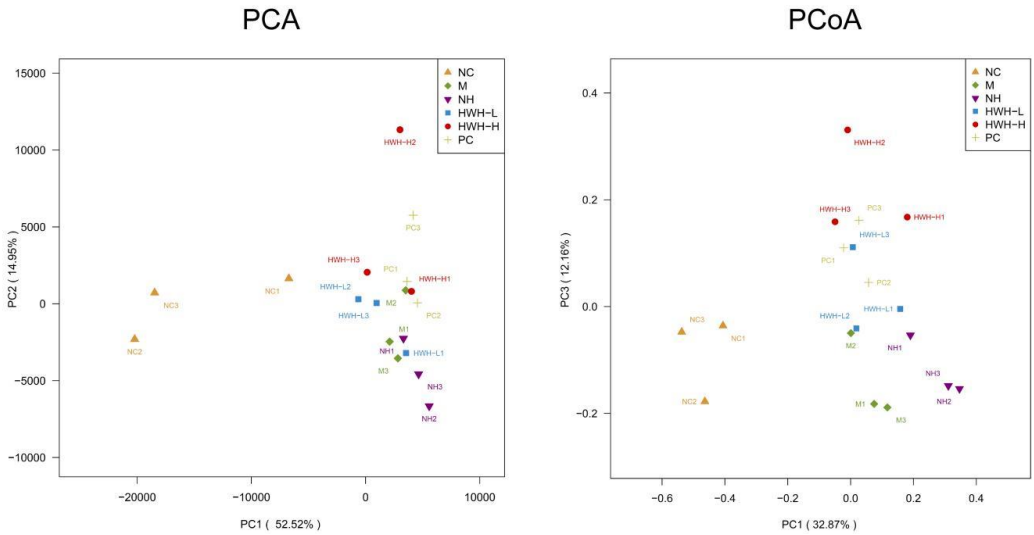

Figure 7. Effects of HWH on beta diversity in CTX-induced immunocompromised mice. NC: Normal control mice; M: Mice treated with 80 mg/kg CTX alone (CTX); HWH-L: Mice treated with CTX plus HWH (80 mg/kg) (HWH80); HWH-H: Mice treated with CTX plus HWH (240 mg/kg) (HWH240); PC: Mice treated with CTX plus levamisole hydrochloride (40 mg/kg); NH: Mice treated with HWH (240 mg/kg) (N240).

Preprints (www.preprints.org) | NOT PEER-REVIEWED | Posted: 13 July 2023 doi:10.20944/preprints202307.0923.v1

2.8. Effects of HWH on taxonomical analysis of gut microbiota

At the phylum level, the OTUs were classified as 11 phyla. The gut consists of Bacteroidetes and Firmicutes, followed by *Proteobacteria*, *Actinobacteria*, *Deferribacteres*, *Chloroflexi*, *Cyanobacteria*, *Gemmatimonadetes*, *Saccharibacteria*, *Tenericutes*, and *Verrucomicrobia*. Compared with NC group, there was a decrease in Firmicutes (M: 74.18% vs. NC: 28.34%) and increase in Bacteroidetes (M: 69.25% vs. NC: 18.3%). In addition, HWH-L group demonstrated an increase in the abundance of Actinobacteria, and drops in the proportions of *Proteobacteria* and *Saccharibacteria* as compared to CTX group (M) (Table S4). CTX treatment decreased the proportion of *Firmicutes* compared to NC group, whereas the HWH intervention increased the abundance of *Firmicutes* as compared to M group (Figure 8A). At genus level, CTX treatment increased the abundance of *Ruminococcus*, and decreased *Lactobacillus*, *Lachnospiraceae*, and *Bifidobacterium*. In contrast, HWH intervention reversed these changes, *Ruminococcus* downregulated, and *Lactobacillus*, *Lachnospiraceae*, and *Bifidobacterium* upregulated (Figure 8B). These outcomes implied that HWH treatment improved the gut microbiota community in CTX-induced immunocompromised mice.

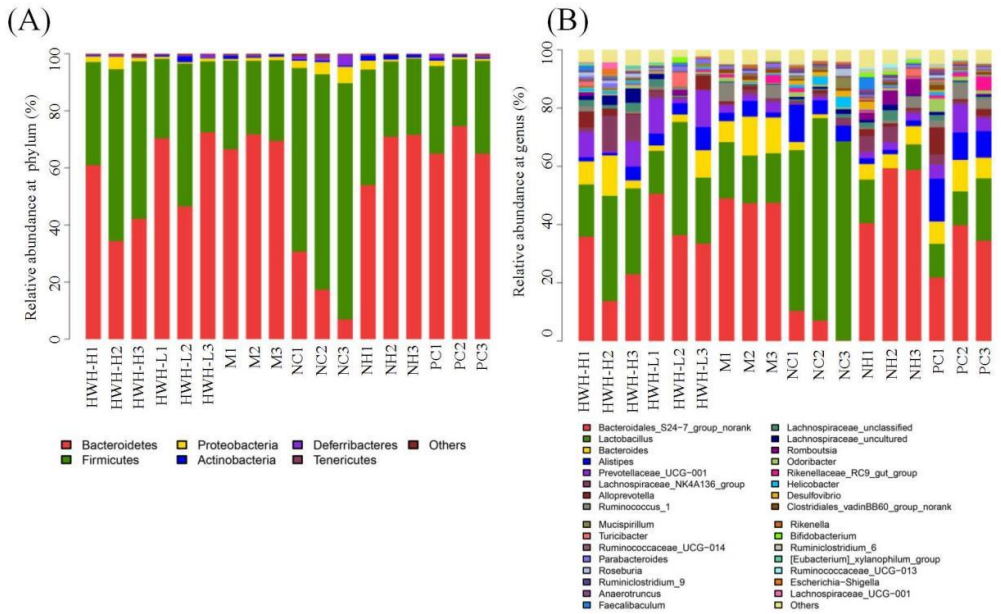

Figure 8. Effects of HWH on microbial community composition at different taxonomy levels in CTX-induced immunocompromised mice. Relative abundance (%) at Phylum level (A). Genus level (B). NC: Normal control mice; M: Mice treated with 80 mg/kg CTX alone (CTX); HWH-L: Mice treated with CTX plus HWH (80 mg/kg) (HWH80); HWH-H: Mice treated with CTX plus HWH (240 mg/kg) (HWH240); PC: Mice treated with CTX plus levamisole hydrochloride (40 mg/kg); NH: Mice treated with HWH (240 mg/kg) (N240).

2.9. Effects of HWH on phylotypes of gut microbiota

LDA results (Figure 9A) demonstrated twenty discriminative features in NC group, and *Bacillus* and *Lactobacillus* were the main microbiota. CTX group (M) showed ten dominant microorganisms as well, and the major microbes were *Clostridiales*, *Staphylococcus*, and *Streptococcus*. HWH-L group displayed two key microorganisms, *Prevotellaceae* and *Christensenellaceae*. HWH-H group displayed eleven discriminative microbes, including *Clostridia*, *Clostridiales*, *Lactobacillus*, etc. PC group showed five dominant microorganisms, *Rikenellaceae* and *Alistipes* were the major microbiota. N240 group (NH) exhibited five dominant phylotypes, including *Bacteroidales*. In cladogram (Figure 9B), *Lactobacillus* had the highest abundance in the purple part which represented NC group. *Clostridiales* exhibited the highest abundance in the marine blue which represented HWH-H group. Overall, these findings suggested that HWH intervention altered the key phylotypes of gut microbiota in CTX-treated mice, and promoted the growth of specific bacteria.

Preprints (www.preprints.org) | NOT PEER-REVIEWED | Posted: 13 July 2023 doi:10.20944/preprints202307.0923.v1

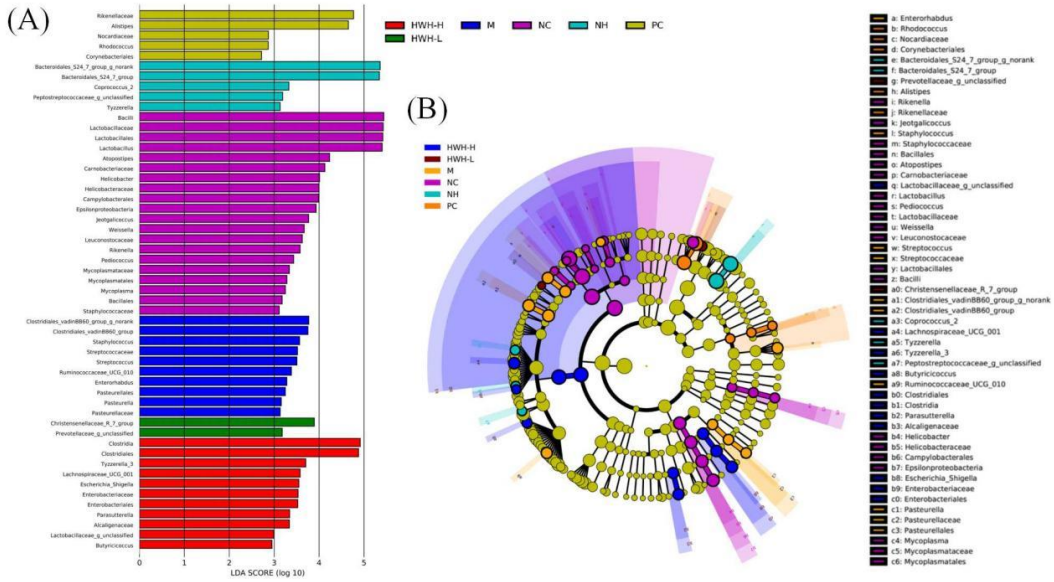

Figure 9. Effects of HWH on key phylotypes of gut microbiota in CTX-induced immunocompromised mice. LDA score (A). LEfSe taxonomic cladogram (B). NC: Normal control mice; M: Mice treated with 80 mg/kg CTX alone (CTX); HWH-L: Mice treated with CTX plus HWH (80 mg/kg) (HWH80); HWH-H: Mice treated with CTX plus HWH (240 mg/kg) (HWH240); PC: Mice treated with CTX plus levamisole hydrochloride (40 mg/kg); NH: Mice treated with HWH (240 mg/kg) (N240).

3. Discussion

Metabolites of CTX can produce the cytotoxic activity. CTX alters the microbial community composition in the colon and damages the intestinal mucosal immunity [35]. It was reported that immunosuppression could damage the intestinal mucosal integrity through decreasing the expression of TJs [36]. Those previous findings indicated that unipotent immune stimulator could not match immunocompromised hosts, and it is required to find a multipotent immune agonist with properties normalizing the gut dysbiosis and repairing the impaired intestinal mucosa.

Some biologically active compounds isolated from sea cucumbers stimulated the body's immune response through activating immune cells. An acidic mucopolysaccharide effectively inhibited the growth of hepatocellular carcinoma through the stimulation of immune organs and tissue proliferation, leading to the enhancement of cellular immunity pathways [37]. Sulfated polysaccharide benefited the host health via modulating gut microbiota composition [31]. While a sea cucumber polysaccharide reduced the intestinal barrier damage, inhibited the inflammatory response, and improved the intestinal microbiota, which was relevant to the production of SCFA [32]. Additionally, sea cucumber peptide exhibited potential antiallergic activities by regulating intestinal microbiota diversity and upregulating the immune response of T lymphocyte subpopulations [38]. In the studies of immune system, spleen indices are significant indicators reflexing immune functions because the spleen is an important immune organ [39]. *Apostichopus japonicus* glycosaminoglycan promoted lymphocyte proliferation in spleen [40]. In addition to its ability to promote splenic lymphocyte proliferation, spleen indices served as a parameter to indicate splenic immune function. Our findings showed that the immune dysfunction induced by CTX was reflected by a significant drop in the spleen indices, which were reversed by HWH intervention.

Cytokines are secreted by immunocytes and non-immune cells which regulate immune functions. It has been reported that the CTX-induced immunosuppression could inhibit the secretions of immune cytokines, including TNF-α [41], IL-6 [42], and IL-1β [43]. TNF-α killed tumor cells directly, and promoted the formation of cytotoxic lymphocytes and the activity of macrophage [36]. IL-6, a pyrogen similar to IL-1 and TNF-α, mediated the acute phase response characterized by leukocytosis and increased acute phase reactants [44]. IL-1β, the major endogenous pyrogen, possessed multiple properties in the response to infection, injury and immune alteration [45]. The

productions of cytokines, specifically TNF-α, IL-6 and IL-1β in macrophage cell line RAW264.7 were enhanced by water-soluble sulfated fucan from the sea cucumber A. leucoprocta [46]. Likewise the expressions of TNF-α and IL-6 were upregulated by *Holothuria leucospilota* polysaccharides in CTX-induced immunosuppressed mice [47]. Secretions of TNF-α, IL-6, and IL-1β in the colon were investigated in this study. The results demonstrated that CTX-treated mice showed significant decline in the generation of IL-6. The administration of HWH (240 mg/kg) showed increased secretions of TNF-α, IL-6, and IL-1β as compared with the CTX group, whereas HWH 80 and PC groups exhibited significantly increased secretions of IL-6 and IL-1β. These results are consistent with those in the previous studies. Overall, HWH could stimulate immune function through increasing the secretions of cytokines.

Mucus, which secreted by goblet cells in the colon, served as a crucial protective indicator against pathogens [48]. Goblet cells could synthesize and secret mucin to the intestinal lumen. Furthermore, mucins were a family of large, complex, glycosylated proteins, and the glycan chain of the mucin could be stained by PAS [49, 50]. After fermentation, *Holothuria leucospilota* polysaccharides were observed to increase the goblet cell count in histological analysis [51]. To investigate the effect of HWH intervention on the CTX-induced immunosuppression driven intestinal mucosal injury, we elucidated the changes in colon histology, intestinal permeability, and microbial composition. The results demonstrated that CTX-induced immunosuppression altered the gut morphology. The histological analysis exhibited inflammatory cell infiltration, loss of crypts, and lower goblet cells in CTX-treated group, whereas HWH treatment improved gut morphology. In addition, the PAS-staining section showed that decreased mucin in the goblet cells were observed in the CTX group, while HWH intervention promoted the expression of mucins in the goblet cells.

TJs in intestinal epithelial cells consisted of different components, including claudin, occludin and ZO-1 [52], which maintained the integrity of the intestinal barrier [53, 54]. A previous study observed that dietary fucoidan of *Acaudina molpadioides* could increase the mRNA of occludin in CTX-treated mice intestine [55]. Although there is limited research about the effects of sea cucumber on TJs, the correlation between intestinal immune function and intestinal integrity is widely acknowledged [56]. Therefore, we investigated the effects of HWH on TJs in this study. Results showed that CTX-induced immunosuppression led to decreased the expressions of TJs, which were reversed by the administration of HWH, indicating that HWH could upregulate the expression of occludin. In the assessments of claudin and ZO-1, CTX group displayed a significant drop in the expressions compared with the NC group. HWH80, HWH240, and PC groups upregulated the expressions of claudin and ZO-1 significantly compared to the CTX group, suggesting that HWH could repair the immunosuppression-induced damage to intestinal physical integrity.

Gut microbiota played crucial roles in modulating host's immune system [57]. Recently, a variety of natural products have been proved to have the ability of regulating gut microbiota [58]. Long-chain bases from sea cucumber could significantly increase Shannon index and decrease in Simpson index, implying that the increased diversity of the gut microbiota [59]. Meanwhile, sulfated polysaccharide could also improve Chao1 and Ace index, implying improved richness and diversity of gut microbiota [60]. We investigated the effect of HWH on the CTX-treated mice gut microbiota with 16S rRNA sequencing. HWH could ameliorate the gut dysbiosis in CTX-induced immunosuppression by alpha diversity analysis. Chao and ACE indices increased in HWH group as compared to CTX croup. Moreover, the number of OTUs also exhibited an increasing trend of microbial community diversity after HWH administration compared to CTX group. Beta diversity analysis (PCA and PCoA) revealed that there was an obvious difference between NC and CTX groups in the overall microbial community structure. Similar observation could be seen between the CTX and HWH-H groups.

Firmicutes and *Bacteroidetes* dominated the gut microbiotas [61], accounting for more than 90% of the microbiota. In the NC group, the proportion of *Firmicutes* was greater than that of *Bacteroidetes*, whereas the CTX disturbed the gut microflora obviously, lowered the proportion of *Firmicutes*. However, HWH intervention increased the proportion of *Firmicutes* compared to CTX group, resulting in increased *Firmicutes*/*Bacteroidetes* (F/B) ratio. A recent study has reported that high salt

 doi:10.20944/preprints202307.0923.v1

feeding mice contained reduced F/B and disrupted immunological response characterized by disturbed immune-related gene expression in the colon [62], which might account for decreased F/B in the CTX-induced immunosuppression. In addition, HWH-L group demonstrated a rise in the abundance of *Actinobacteria* and declines in the proportions of *Proteobacteria*, a microbial marker of gut dysbiosis [63] and *Saccharibacteria* compared with CTX group. The administration of fucoidan ectracted from sea cucumber *Pearsonothuria graeffei* could lead to an increase in the abundances of *Bacteroidetes* and *Actinobacteria* while decreasing the richness of *Firmicutes* and *Proteobacteria* [64]. *Saccharibacteria*, known as TM7, has been reported an association with the inflammatory bowel diseases (IBDs). It played an important role as promoters of inflammation in the early stages of inflammatory mucosal processes by triggering inflammation directly or modifying growth conditions for competing bacterial populations [65]. *Bifidobacterium* and *Lactobacillus* were widely used as benchmark for evaluating the effect of prebiotics, containing lots of beneficial properties for the host. For example, both RG I (potato galactan-rich rhamnogalacturonan I) and its corresponding oligosaccharides/oligomers showed their prebiotic properties by stimulating the growth of *Bifidobacterium* spp. and *Lactobacillus* spp. [66]. *Lactobacillus* was promoted with chitosan treatment in DSS-induced ulcerative colitis mice [34]. While *Ruminococcus* are linked to IBDs usually. Previous reports revealed how some strains of *Ruminococcus* could drive the inflammatory responses that characterize IBD [67]. Amounts of *Enterobacteriaceae* and *Ruminococcus gnavus* increased, and *Faecalibacterium* and *Roseburia* disappeared in IBDs [68]. Similarly in the rats' obesity model, the relative abundance of *Romboutsia*, *Ruminococcus*, *Corynebacteriume*, and *Saccharibacteria* groups increased brought about high-fat diet (HFD), and the above upregulation were significantly reversed by the intervention of winter melon and lotus leaf Tibetan tea [69]. Alterations in abundance of microorganisms may cause changes in some metabolic pathways, in addition to altering the biosynthesis and degradation of some secondary metabolites, which are mostly associated with diseases. In our work, *Bifidobacterium* and *Lactobacillus* decreased after the CTX treatment. HWH intervention improved the structure of the gut microbiota induced by CTX, increased *Bifidobacterium* and *Lactobacillus* compared to CTX group, while significantly decreasing *Ruminococcus* and *Saccharibacteria*.

Moreover, LEfSe analysis results indicated that the key phylotypes in NC group were *Lactobacillus*, *Lactobacillaceae*, *Lactobacillales* which belongs to beneficial bacteria of gut microbiota. *Lactobacillus* were particularly characterized in the protection from pathogenic bacteria, modulation of the immune system to potentially reduced risk of allergies and cancer, reduction of radical oxidative species and cholesterol levels, and potentially benefiting in diabetes [70]. *Lactobacillus* also strengthened intestinal barrier function, promoted TJ integrity, and protected against experimental necrotizing enterocolitis [71]. The discriminative microbes of CTX group involved *Staphylococcus* and *Streptococcus* which can serve as conditioned pathogens [72, 73]. Above microbes may pose a serious threat for the human or animal host when they get access to inner layers of the body through breaches in skin or membranes [74, 75]. The family *Christensenellaceae* showed compelling associations with host health which suggested that the cultured *Christensenellaceae* could be considered as a therapeutic probiotic to improve human health [76]. The results demonstrated that the gut microbiota of NC group was dominated by beneficial bacteria such as *Lactobaccilus* which disappeared in CTX group. The harmful bacteria in CTX group including *Staphylococcus* and *Streptococcus* which vanished in the HWH-L and HWH-H groups. Then, *Christensenellaceae* dominated the gut microflora of HWH-L group. Therefore, CTX caused a change in the gut microbiota composition, inhibited the growth of beneficial bacteria and promoted the growth of harmful bacteria, while the intervention of HWH could reverse this trend. HWH had an excellent ability to regulate the disturbance of gut microbiota caused by CTX.

4. Materials and Methods

4.1. Materials and reagents

 doi:10.20944/preprints202307.0923.v1

HWH was supplied and analyzed by Zhen Jiu Co., Ltd. (Dalian, China). Cyclophosphamide was purchased from Aladdin (Shanghai, China). Levamisole hydrochloride was purchased from Shanxi Hongbao Veterinary Pharmaceutical Co., Ltd. (Shanxi, China). The First Strand cDNA Synthesis Kit and the SYBR PrimeScript™ RT-PCR Kit were purchased from Takara Bio Co., Ltd. (Shiga, Japan). The primer sequences of TNF-α, IL-6 and IL-1β were synthesized by Sangon Biotech Co., Ltd. (Shanghai, China). Primary antibody against occludin was purchased from Proteintech Group Co., Ltd. (Wuhan, China). Antibodies against claudin and ZO-1 were from Wanleibio Co., Ltd. (Shenyang, China). E.Z.N.A.® Stool DNA Kit was purchased from Omega Bio-Tek Co., Ltd. (Georgia, USA). AxyPrep DNA Gel Extraction Kit was purchased from Axygen, Inc. (NY, USA).

4.2. Preparation of HWH

HWH was derived from sea cucumber via enzymatic hydrolysis and produced by Dalian Zhenjiu Biological Industry Co., Ltd. Briefly, the sea cucumbers were cleaned after gutting, and thoroughly crushed by a blender, hydrolyzed with a neutral protease (3000 U/g), precipitated, filtrated, and dried to obtain HWH.

4.3. Composition determination of HWH

The moisture content of HWH was measured by using the direct drying method. The ash content of HWH was measured by using the high-temperature ashing method. The total protein content of HWH was determined by the Kjeldahl method [77]. Total carbohydrate content of HWH was determined by phenol-H_2SO_4 method [78].

4.4 Identification of peptides in HWH by LC-MS

A 2% HWH solution was prepared and centrifuged in an ultrafiltration tube with an interception capacity of 10 kDa. Then, filtrate was collected, and analyzed by Easy-nLC-Orbitrap-MS/MS system (Thermo Fisher Scientific, Waltham, MA, USA) with a reversed-phase C18 column (0.15 × 120 mm, 1.9 μm) at nano-flow gradient (flow rate, 600 nL min^{-1}). The mobile phase A was composed of ultrapure water (containing 0.1% formic acid), and the mobile phase B was composed of acetonitrile (containing 0.1% formic acid) with gradient programme of 0-11 min, 93-85% A; 11-48 min, 85-75% A; 48-62 min, 75-60% A. Maxquant_2.0.1.0 software was used for peptide matching. The measured peptides were evaluated by PeptideRanker.

4.5. Animals and experimental design

Female BALB/c mice (weight, 20 ± 2 g) were purchased from Animal Experimental Center of Dalian Medical University, Dalian, China (Certificate of quality number: SCXK (Liao) 2018-0003; 20 May 2018). All experimental procedures were approved by Animal Care and Research Ethics Committee of Dalian Medical University (Approval number: SYXK (Liao) 2018-0006; 18 November 2018). Mice were accommodated in an environmentally controlled room, and had free access to standard diet and water ad libitum. After acclimation for one week, sixty mice were randomly divided into six groups (10 mice in each group), named NC, CTX, HWH80, HWH240, PC (positive control) and N240 (HWH control). Groups NC and N240 received normal saline and 240 mg/kg of HWH respectively, and the other four groups received CTX (80 mg/kg, intraperitoneally) once a day for 3 days to induce immunodeficiency [30]. And then, groups CTX, HWH80, HWH240 and PC were treated with normal saline, 80 mg/kg, 240 mg/kg of HWH [26], and 40 mg/kg of levamisole hydrochloride [35] intragastrically once a day for 7 days. All animals were killed 12 h later to collect fecal samples for microbial composition analysis using 16S rRNA Illumina sequencing. One part of colon and spleen tissues were fixed in 4% paraformaldehyde for histological analysis, and the remaining parts were prepared for Western blotting and qRT-PCR.

4.6. Determination of spleen index

The spleen index was calculated as follows:

Spleen index = spleen weight (mg) / body weight (g) × 100%

 doi:10.20944/preprints202307.0923.v1

4.7. Histological analysis

The distal colon and spleen were dissected, and fixed in 4% paraformaldehyde respectively for 24 h, gradient dehydrated by ethanol, vitrificated by xylene, and embedded in paraffin. Sections of 3 μm thickness were prepared via a microtome (Leica, Germany). Spleen slides were stained with hematoxylin and eosin (H&E) after rehydration. Colon slides were stained with H&E and periodic acid schiff (PAS). Images were obtained using an optical microscope. Spleen and colon samples were observed at 40× and 100× magnification, respectively.

4.8. Western blotting analysis

Total protein was extracted from the colon, and homogenized in RIPA buffer with 1:100 phenylmethylsulfonyl fluoride (PMSF) using ultrasonic extraction: work for 4 s and rest for 4 s (duration at 8 min and power of 10 watts), followed by resting on ice for 30 min and centrifugation at 12000 rpm for 20 min at 4℃ to obtain the supernatant. Protein concentration was determined using a BCA kit according to the manufacturer's instructions. Total protein (20 μg) was fractionated on a 12% SDS-PAGE, and transferred to PVDF membranes for 40 min for β-actin, 30 min for claudin-1, 60 min for occludin, and 180 min for ZO-1 respectively. PVDF membranes were blocked with 5% skimmed milk, and incubated with primary antibodies at a 1:2000 dilution overnight at 4℃, followed by incubation with HRP-conjugated secondary antibodies at a 1:8000 dilution for 2 h at room temperature after washed with TBST for three times. Blots were visualized using ECL kit (Thermo Fisher, USA), and images were captured by ChemiDoc MP imaging system (Bio-Rad, Hercules, CA, USA). β-actin was used as internal reference.

4.9. Quantitative real-time PCR

Total RNA was extracted from colon tissue with TRIzol reagent, and cDNA was obtained by First Strand cDNA Synthesis Kit according to the manufacturer's protocol. Then, the qRT-PCR was performed using the SYBR PrimeScript™ RT-PCR Kit (Takara). Data were analyzed using $2^{-\Delta\Delta Ct}$ method. GAPDH was used as an internal control. Primer sequences used were shown in Table S1.

4.10. 16 S rRNA sequencing of gut microbiota

Total DNA was extracted from fecal samples using E.Z.N.A.® Stool Kit. The V3-V4 regions of bacterial 16S rRNA gene was amplified by PCR with primers 338F (5'-ACTCCTACGGGAGGCAGCA-3') and 806R (5'-GGACTACHVGGGTWTCTAAT-3'), and the following protocol: initial denaturation at 98℃ for 1 min, followed by 30 cycles of denaturation at 98 ℃ for 10 s, annealing at 50℃ for 30 s, elongation at 72℃ for 1 min, and a final extension at 72℃ for 5 min. The PCR products were separated and detected on a 2% agarose gel, purified by AxyPrep DNA Gel Extraction Kit, and quantified with Quantifluor dsDNA quantification system. The amplicons were normalized, pooled and sequenced on the Illumina NovaSeq PE250. The sequencing library was generated using NEB Next®Ultra™DNA Library Prep Kit for Illumina (NEB, USA). The library quality was assessed on the Qubit®2.0 Fluorometer (Thermo Scientific, USA) and Agilent Bioanalyzer 2100 system (Agilent, USA). Quality sequences were acquired by removing low-quality reads. Taxonomic assignment was performed using the SILVA 132. Operational taxonomic units (OTUs) were generated using Usearch vsesion 10 with a dissimilarity cutoff of 0.03. Alpha diversity was calculated with mothur v.1.30 and beta diversity was analyzed using Quantitative Insights into Microbial Ecology (QIIME) with weighted and unweighted Unifrac distance matrix to measure similarity in microbial composition between samples. Bacterial relative abundance was analyzed and performed by QIIME and R software. The linear discriminant analysis (LDA) and LDA effect size (LEfSe) methods were used to quantify biomarkers within different groups with statistical significance.

4.11. Statistical analysis

GraphPad Prism 8.0.1 (La Jolla, CA, USA) was used for analysis. A one-way analysis of variance (ANOVA) was performed with Tukey's multiple comparison test to determine the significance of differences, and p-value < 0.05 was considered significant.

5. Conclusions

HWH could improve the immune function, repair the impaired intestinal mucosal integrity, and regulate the diversity and composition structure of gut microbiota in CTX-induced immunosuppression. HWH regulated the gut microbiota by restoring *Lactobacillus*, *Lachnospiraceae*, *Christensenellaceae*, and *Bifidobacterium*, and decreasing *Ruminococcus*, *Staphylococcus*, and *Streptococcus* in CTX-treated mice. Additionally, HWH could increase the spleen indices and stimulate the secretions of TNF-α, IL-1β, and IL-6 in the colon. HWH improved intestinal barrier, restored the goblet cells in the crypt of the colon, and upregulated the expressions of TJs. These findings suggested that HWH had the potential as an effective immunomodulator, a prebiotic, and an intestinal mucosal repair agent. Detailed mechanisms of HWH on mitigating intestinal mucosal immunity and gut microbiota remain to be investigated. Development of sea cucumber based functional foods is the future perspectives in this field, several factors such as the organoleptic property, bio-accessibility, bioavailability, and personally designed products, need to be considered. Meanwhile the production, extraction and purification of active ingredients from sea cucumber at a large scale are another concerns for researchers.

Supplementary Materials: The following supporting information can be downloaded at the website of this paper posted on Preprints.org. Table S1: The forward primer and reverse primer for qRT-PCR. Table S2: Summary of OTUs sequencing data. Table S3: Summary of alpha diversity indices estimation. Table S4: Percentage of bacterial phyla in experimental groups. The sequencing data were deposited in the NCBI Database (Accession number: PRJNA932944). Database URL: https://www.ncbi.nlm.nih.gov/sra/PRJNA932944.

Author Contributions: Conceptualization, B.F. and XL.L.; methodology, C.Y. and HR.Q.; software, C.Y.; validation, XL.L. and C.Y.; formal analysis, C.Y.; investigation, C.Y. and HR.Q.; resources, XL.L.; data curation, C.Y. and B.F.; writing—original draft preparation, C.Y., HR.Q. and XL.L.; writing—review and editing, B.F. and XL.L.; supervision, B.F.; project administration, XL.L.; funding acquisition, XL.L. All authors have read and agreed to the published version of the manuscript.

Funding: This research was funded by Liaoning Natural Science Foundation of China, grant number 2021-MS-289.

Institutional Review Board Statement: The animal study protocol was approved by Animal Care and Research Ethics Committee of Dalian Medical University (protocol code SYXK (Liao) 2018-0006; 18 November 2018).

Data Availability Statement: The original contributions presented in the study are included in the article/Supplementary material;, further inquiries can be directed to the corresponding authors.

Acknowledgments: This work was supported by Liaoning Natural Science Foundation of China, (grant number 2021-MS-289). The authors thank the staffs of the College of Basic Medical Sciences in Dalian Medical University. We would like to thank Jing Lan of Dalian Zhenjiu Biological Industry Co., Ltd for the chemical composition analysis of HWH.

Conflicts of Interest: The authors declare no conflict of interest.

References

1. Etienne-Mesmin, L.; Chassaing, B.; Desvaux, M.; De Paepe, K.; Gresse, R.; Sauvaitre, T.; Forano, E.; Van de Wiele, T.; Schüller, S.; Juge, N.; Blanquet-Diot, S. Experimental models to study intestinal microbes-mucus interactions in health and disease. *FEMS Microbiol. Rev.* **2019**, *43*, 457-489.
2. Lynch, S.V.; Pedersen, O. The human intestinal microbiome in health and disease. *N. Engl. J. Med.* **2016**, *375*, 2369-2379.
3. Eckburg, P.B.; Bik, E.M.; Bernstein, C.N.; Purdom, E.; Dethlefsen, L.; Sargent, M.; Gill, S.R.; Nelson, K.E.; Relman, D.A. Diversity of the human intestinal microbial flora. *Science* **2005**, *308*, 1635-1638.
4. Reyes, A.; Haynes, M.; Hanson, N.; Angly, F.E.; Heath, A.C.; Rohwer, F.; Gordon, J.I. Viruses in the faecal microbiota of monozygotic twins and their mothers. *Nature* **2010**, *466*, 334-338.
5. Zmora, N.; Suez, J.; Elinav, E. You are what you eat: diet, health and the gut microbiota. *Nat. Rev. Gastroenterol. Hepatol.* **2019**, *16*, 35-56.

6. Franzosa, E.A.; Huang, K.; Meadow, J.F.; Gevers, D.; Lemon, K.P.; Bohannan, B.J.; Huttenhower, C. Identifying personal microbiomes using metagenomic codes. *Proc. Natl. Acad. Sci. USA* **2015**, *112*, E2930-E2938.
7. Patterson, E.; Ryan, P.M.; Cryan, J.F.; Dinan, T.G.; Ross, R.P.; Fitzgerald, G.F.; Stanton, C. Gut microbiota, obesity and diabetes. *Postgrad. Med. J.* **2016**, *92*, 286-300.
8. Turnbaugh, P.J.; Ley, R.E.; Mahowald, M.A.; Magrini, V.; Mardis, E.R.; Gordon, J.I. An obesity-associated gut microbiome with increased capacity for energy harvest. *Nature* **2006**, *444*, 1027-1031.
9. Qin, J.; Li, Y.; Cai, Z.; Li, S.; Zhu, J.; Zhang, F.; Liang, S.; Zhang, W.; Guan, Y.; Shen, D.; et al. A metagenome-wide association study of gut microbiota in type 2 diabetes. *Nature* **2012**, *490*, 55-60.
10. Li, J.; Zhao, F.; Wang, Y.; Chen, J.; Tao, J.; Tian, G.; Wu, S.; Liu, W.; Cui, Q.; Geng, B.; et al. Gut microbiota dysbiosis contributes to the development of hypertension. *Microbiome* **2017**, *5*, 14.
11. Ni, J.; Wu, G.D.; Albenberg, L.; Tomov, V.T. Gut microbiota and IBD: causation or correlation?. *Nat. Rev. Gastroenterol. Hepatol.* **2017**, *14*, 573-584.
12. Vollaard, E.J.; Clasener, H.A. Colonization resistance. *Antimicrob. Agents Chemother.* **1994**, *38*, 409-414.
13. Pickard, J.M.; Zeng, M.Y.; Caruso, R.; Núñez, G. Gut microbiota: Role in pathogen colonization, immune responses, and inflammatory disease. *Immunol. Rev.* **2017**, *279*, 70-89.
14. Antonini, M.; Lo Conte, M.; Sorini, C.; Falcone, M. How the Interplay Between the Commensal Microbiota, Gut Barrier Integrity, and Mucosal Immunity Regulates Brain Autoimmunity. *Front. Immunol.* **2019**, *10*, 1937.
15. Chelakkot, C.; Ghim, J.; Ryu, S.H. Mechanisms regulating intestinal barrier integrity and its pathological implications. *Exp. Mol. Med.* **2018**, *50*, 1-9.
16. Eri, R.; Chieppa, M. Messages from the Inside. The Dynamic Environment that Favors Intestinal Homeostasis. *Front. Immunol.* **2013**, *4*, 323.
17. Saenz, S.A.; Taylor, B.C.; Artis, D. Welcome to the neighborhood: epithelial cell-derived cytokines license innate and adaptive immune responses at mucosal sites. *Immunol. Rev.* **2008**, *226*, 172-190.
18. Paone, P.; Cani, P.D. Mucus barrier, mucins and gut microbiota: the expected slimy partners?. *Gut* **2020**, *69*, 2232-2243.
19. Rinninella, E.; Cintoni, M.; Raoul, P.; Lopetuso, L.R.; Scaldaferri, F.; Pulcini, G.; Miggiano, G.A.D.; Gasbarrini, A.; Mele, M.C. Food Components and Dietary Habits: Keys for a Healthy Gut Microbiota Composition. *Nutrients* **2019**, *11*, 2393.
20. Bian, R.; Tang, J.; Hu, L.; Huang, X.; Liu, M.; Cao, W.; Zhang, H. (E)-phenethyl 3-(3,5-dihydroxy-4-isopropylphenyl) acrylate gel improves DNFB-induced allergic contact hypersensitivity via regulating the balance of Th1/Th2/Th17/Treg cell subsets. *Int. Immunopharmacol.* **2018**, *65*, 8-15.
21. Hu, N.; Qu, Y.; Liu, T.Y.; Zhou, Y.; Liu, C.; Wang, J.H.; Yang, B.F.; Li, C.L. Immunomodulatory effects and mechanisms of Tiepishihu Xiyangshen granules on cyclophosphamide induced immuno-suppression via TLR4/MAPKs and PI3K/AKT/FOXO3a signal pathways. *J. Ethnopharmacol.* **2023**, *307*, 116192.
22. Rehman, A.U.; Siddiqui, N.Z.; Farooqui, N.A.; Alam, G.; Gul, A.; Ahmad, B.; Asim, M.; Khan, A.I.; Xin, Y.; Zexu, W.; et al. Morchella esculenta mushroom polysaccharide attenuates diabetes and modulates intestinal permeability and gut microbiota in a type 2 diabetic mice model. *Front. Nutr.* **2022**, *9*, 984695.
23. Han, X.; Bai, B.; Zhou, Q.; Niu, J.; Yuan, J.; Zhang, H.; Jia, J.; Zhao, W.; Chen, H. Dietary supplementation with polysaccharides from Ziziphus Jujuba cv. Pozao intervenes in immune response via regulating peripheral immunity and intestinal barrier function in cyclophosphamide-induced mice. *Food Funct.* **2020**, *11*, 5992-6006.
24. Khotimchenko, Y. Pharmacological potential of sea cucumbers. *Int. J. Mol. Sci.* **2018**, *19*, 1342.
25. Lobine, D.; Rengasamy, K.R.R.; Mahomoodally, M.F. Functional foods and bioactive ingredients harnessed from the ocean: current status and future perspectives. *Crit. Rev. Food. Sci. Nutr.* **2022**, *62*, 5794-5823.
26. Zheng, R.; Li, X.; Cao, B.; Zuo, T.; Wu, J.; Wang, J.; Xue, C.; Tang, Q. Dietary Apostichopus japonicus enhances the respiratory and intestinal mucosal immunity in immunosuppressive mice. *Biosci. Biotechnol. Biochem.* **2015**, *79*, 253-259.
27. Aminin, D.L.; Silchenko, A.S.; Avilov, S.A.; Stepanov, V.G.; Kalinin, V.I. Immunomodulatory action of monosulfated triterpene glycosides from the sea cucumber Cucumaria okhotensis: stimulation of activity of mouse peritoneal macrophages. *Nat. Prod. Commun.* **2010**, *5*, 1877-1880.
28. Aminin, D.L.; Agafonova, I.G.; Kalinin, V.I.; Silchenko, A.S.; Avilov, S.A.; Stonik, V.A.; Collin, P.D.; Woodward, C. Immunomodulatory properties of frondoside A, a major triterpene glycoside from the North Atlantic commercially harvested sea cucumber Cucumaria frondosa. *J. Med. Food* **2008**, *11*, 443-453.
29. Silchenko, A.S.; Kalinovsky, A.I.; Avilov, S.A.; Andryjaschenko, P.V.; Dmitrenok, P.S.; Menchinskaya, E.S.; Aminin, D.L.; Kalinin, V.I. Structure of cucumarioside I2 from the sea cucumber Eupentacta

fraudatrix (Djakonov et Baranova) and cytotoxic and immunostimulatory activities of this saponin and relative compounds. *Nat. Prod. Res.* **2013**, *27*, 1776-1783.
30. Niu, Q.; Li, G.; Li, C.; Li, Q.; Li, J.; Liu. C.; Pan, L.; Li, S.; Cai, C.; Hao, J.; et al. Two different fucosylated chondroitin sulfates: Structural elucidation, stimulating hematopoiesis and immune-enhancing effects. *Carbohydr Polym.* **2020**, *230*, 115698.
31. Liu, Z.; Zhang, Y.; Ai, C.; Wen, C.; Dong, X.; Sun, X.; Cao, C.; Zhang, X.; Zhu, B.; Song, S. Gut microbiota response to sulfated sea cucumber polysaccharides in a differential manner using an in vitro fermentation model. *Food Res. Int.* **2021**, *148*, 110562.
32. Wang, Z.; Shi, Y.; Zeng, S.; Zheng, Y.; Wang, H.; Liao, H.; Song, J.; Zhang, X.; Cao, J.; Li, C. Polysaccharides from *Holothuria leucospilota* relieve loperamide-induced constipation symptoms in mice. *Int. J. Mol. Sci.* **2023**, *24*, 2553.
33. Wang, X.; Sun, G.; Feng, T.; Zhang, J.; Huang, X.; Wang, T.; Xie, Z.; Chu, X.; Yang, J.; Wang, H.; et al. Sodium oligomannate therapeutically remodels gut microbiota and suppresses gut bacterial amino acids-shaped neuroinflammation to inhibit Alzheimer's disease progression. *Cell Res.* **2019**, *29*, 787-803.
34. Wang, J.; Zhang, C.; Guo, C.; Li, X. Chitosan Ameliorates DSS-Induced Ulcerative Colitis Mice by Enhancing Intestinal Barrier Function and Improving Microflora. *Int. J. Mol. Sci.* **2019**, *20*, 5751.
35. Ying, M.; Yu, Q.; Zheng, B.; Wang, H.; Wang, J.; Chen, S.; Nie, S.; Xie, M. Cultured Cordyceps sinensis polysaccharides modulate intestinal mucosal immunity and gut microbiota in cyclophosphamide-treated mice. *Carbohydr. Polym.* **2020**, *235*, 115957.
36. Zhao, Y.; Yan, Y.; Zhou, W.; Chen, D.; Huang, K.; Yu, S.; Mi, J.; Lu, L.; Zeng, X.; Cao, Y. Effects of polysaccharides from bee collected pollen of Chinese wolfberry on immune response and gut microbiota composition in cyclophosphamide-treated mice. *J. Funct. Foods* **2020**, *72*, 104057.
37. Song, Y.; Jin, S.J.; Cui, L.H.; Ji, X.J.; Yang, F.G. Immunomodulatory effect of *Stichopus japonicas* acid mucopolysaccharide on experimental hepatocellular carcinoma in rats. *Molecules* **2013**, *18*, 7179-7193.
38. Yun, L.; Li, W.; Wu, T.; Zhang, M. Effect of sea cucumber peptides on the immune response and gut microbiota composition in ovalbumin-induced allergic mice. *Food Funct.* **2022**, *13*, 6338-6349.
39. Meng, M.; Wang, H.; Li, Z.; Guo, M.; Hou, L. Protective effects of polysaccharides from Cordyceps gunnii mycelia against cyclophosphamide-induced immunosuppression to TLR4/TRAF6/NF-κB signalling in BALB/c mice. *Food Funct.* **2019**, *10*, 3262-3271.
40. Wang, H.; Yang, S.; Wang, Y.; Jiang, T.; Li, S.; Lv, Z. Immunoenhancement effects of glycosaminoglycan from Apostichopus japonicus: In vitro and in cyclophosphamide-induced immunosuppressed mice studies. *Mar. drugs* **2017**, *15*, 347.
41. Zhu, Z.; Zhu, B.; Sun, Y.; Ai, C.; Wu, S.; Wang, L.; Song, S.; Liu, X. Sulfated polysaccharide from sea cucumber modulates the gut microbiota and its metabolites in normal mice. *Int. J. Biol. Macromol*. **2018**, *120*, 502-512.
42. Kim, J.K.; Kim, J.Y.; Jang, S.E.; Choi, M.S.; Jang, H.M.; Yoo, H.H.; Kim, D.H. Fermented red ginseng alleviates cyclophosphamide-induced immunosuppression and 2,4,6-trinitrobenzenesulfonic acid-induced colitis in mice by regulating macrophage activation and T cell differentiation. *Am. J. Chin. Med.* **2018**, *46*, 1879-1897.
43. Yoo, J.H.; Lee, Y.S.; Ku, S.; Lee, H.J. Phellinus baumii enhances the immune response in cyclophosphamide-induced immunosuppressed mice. *Nutr. Res.* **2020**, *75*, 15-31.
44. Schulte, W.; Bernhagen, J.; Bucala, R. Cytokines in sepsis: potent immunoregulators and potential therapeutic targets--an updated view. *Mediators. Inflamm.* **2013**, *2013*, 165974.
45. Dinarello, C.A. Interleukin-1 and the pathogenesis of the acute-phase response. *N. Engl. J. Med.* **1984**, *311*, 1413-1418.
46. Feng, G.; Laijin, S.; Chen, S.; Teng, W.; Dejian, Z.; Yin, C.; Shoudong, G. In vitro and in vivo immunoregulatory activity of sulfated fucan from the sea cucumber A. leucoprocta. *Int. J. Biol. Macromol.* **2021**, *187*, 931-938.
47. Zhao, F.; Ma, T.; Zhang, X.; Zhao, Q.; Zhu, K.; Cao, J.; Liu, Z.; Shen, X.; Li, C. Holothuria leucospilota polysaccharides improve immunity and the gut microbiota in cyclophosphamide-treated immunosuppressed mice. *Mol. Nutr. Food Res*. **2023**, *67*, e2200317.
48. Wlodarska, M.; Thaiss, C.A.; Nowarski, R.; Henao-Mejia, J.; Zhang, J.P.; Brown, E.M.; Frankel, G.; Levy, M.; Katz, M.N.; Philbrick, W.M.; et al. NLRP6 inflammasome orchestrates the colonic host-microbial interface by regulating goblet cell mucus secretion. *Cell* **2014**, *156*, 1045-1059.
49. Siddiqui, N.Z.; Rehman, A.U.; Yousuf, W.; Khan, A.I.; Farooqui, N.A.; Zang, S.; Xin, Y.; Wang, L. Effect of crude polysaccharide from seaweed, Dictyopteris divaricata (CDDP) on gut microbiota restoration and anti-diabetic activity in streptozotocin (STZ)-induced T1DM mice. *Gut Pathog.* **2022**, *17*, 39.
50. Vemuri, R.; Gundamaraju, R.; Shinde, T.; Perera, A.P.; Basheer, W.; Southam, B.; Gondalia, S.V.; Karpe, A.V.; Beale, D.J.; Tristram, S.; et al. *Lactobacillus acidophilus* DDS-1 modulates intestinal-specific microbiota, short-chain fatty acid and immunological profiles in aging mice. *Nutrients* **2019**, *11*, 1297.

51. Wang, W.; Yuan, Y.; Cao, J.; Shen, X.; Li, C. Beneficial effects of *Holothuria leucospilota* polysaccharides on fermentability in vivo and in vitro. *Foods* **2021**, *10*, 1884.
52. Suzuki, T. Regulation of the intestinal barrier by nutrients: The role of tight junctions. *Anim. Sci. J.* **2020**, *91*, e13357.
53. Noth, R.; Lange-Grumfeld, J.; Stüber, E.; Kruse, M.L.; Ellrichmann, M.; Häsler, R.; Hampe, J.; Bewig, B.; Rosenstiel, P.; Schreiber, S; et al. Increased intestinal permeability and tight junction disruption by altered expression and localization of occludin in a murine graft versus host disease model. *BMC Gastroenterol.* **2011**, *11*, 109.
54. Bai, Y.; Huang, F.; Zhang, R.; Dong, L.; Jia, X.; Liu, L.; Yi, Y.; Zhang, M. Longan pulp polysaccharides relieve intestinal injury in vivo and in vitro by promoting tight junction expression. *Carbohydr. Polym.* **2020**, *229*, 115475.
55. Shi, H.; Chang, Y.; Gao, Y.; Wang, X.; Chen, X.; Wang, Y.; Xue, C.; Tang, Q. Dietary fucoidan of Acaudina molpadioides alters gut microbiota and mitigates intestinal mucosal injury induced by cyclophosphamide. *Food Funct*. **2017**, *8*, 3383-3393.
56. Goto, Y. Epithelial cells as a transmitter of signals from commensal bacteria and host immune cells. *Front. Immunol.* **2019**, *10*, 2057.
57. Ramakrishna, B.S. Role of the gut microbiota in human nutrition and metabolism. *J. Gastroenterol. Hepatol.* **2013**, *28*, 9-17.
58. Shang, Q.; Jiang, H.; Cai, C.; Hao, J.; Li, G.; Yu, G. Gut microbiota fermentation of marine polysaccharides and its effects on intestinal ecology: An overview. *Carbohydr. Polym.* **2018**, *179*, 173-185.
59. Hu, S.; Xu, Y.; Gao, X.; Li, S.; Jiang, W.; Liu, Y.; Su, L.; Yang, H. Long-chain bases from sea cucumber alleviate obesity by modulating gut microbiota. *Mar. drugs* **2019**, *17*, 455.
60. Zhu, G.; Luo, J.; Du, H.; Jiang, Y.; Tu, Y.; Yao, Y.; Xu, M. Ovotransferrin enhances intestinal immune response in cyclophosphamide-induced immunosuppressed mice. *Int. J. Biol. Macromol.* **2018**, *120*, 1-9.
61. Pushpanathan, P.; Mathew, G.S.; Selvarajan, S.; Seshadri, K.G.; Srikanth, P. Gut Microbiota and its mysteries. *Indian J. Med. Microbiol.* **2019**, *37*, 268-277.
62. Hu, J.; Luo, H.; Wang, J.; Tang, W.; Lu, J.; Wu, S.; Xiong, Z.; Yang, G.; Chen, Z.; Lan, T.; et al. Enteric dysbiosis-linked gut barrier disruption triggers early renal injury induced by chronic high salt feeding in mice. *Exp. Mol. Med.* **2017**, *49*, e370.
63. Shin, N.R.; Whon, T.W.; Bae, J.W. Proteobacteria: microbial signature of dysbiosis in gut microbiota. *Trends Biotechnol.* **2015**, *33*, 496-503.
64. Li, S.; Li, J.; Mao, G.; Wu, T.; Hu, Y.; Ye, X.; Tian, D.; Linhardt, R.J.; Chen, S. A fucoidan from sea cucumber Pearsonothuria graeffei with well-repeated structure alleviates gut microbiota dysbiosis and metabolic syndromes in HFD-fed mice. *Food Funct*. **2018**, *9*, 5371-5380.
65. Kuehbacher, T.; Rehman, A.; Lepage, P.; Hellmig, S.; Fölsch, U.R.; Schreiber, S.; Ott, S.J. Intestinal TM7 bacterial phylogenies in active inflammatory bowel disease. *J. Med. Microbiol.* **2008**, *57*, 1569-1576.
66. Henke, M.T.; Brown, E.M.; Cassilly, C.D.; Vlamakis, H.; Xavier, R.J.; Clardy, J. Capsular polysaccharide correlates with immune response to the human gut microbe Ruminococcus gnavus. *Proc. Natl. Acad. Sci. USA* **2021**, *118*, e2007595118.
67. Khodaei, N.; Fernandez, B.; Fliss, I.; Karboune, S. Digestibility and prebiotic properties of potato rhamnogalacturonan I polysaccharide and its galactose-rich oligosaccharides/oligomers. *Carbohydr. Polym*. **2016**, *136*, 1074-1084.
68. Willing, B.P.; Dicksved, J.; Halfvarson, J.; Andersson, A.F.; Lucio, M.; Zheng, Z.; Järnerot, G.; Tysk, C.; Jansson, J.K.; Engstrand, L. A pyrosequencing study in twins shows that gastrointestinal microbial profiles vary with inflammatory bowel disease phenotypes. *Gastroenterology* **2010**, *139*, 1844-1854.
69. Yuan, Y.; Zhang, B.; He, J.L.; Wei, T.; Liu, D.J.; Yang, W.J.; Guo, C.Y.; Nie, X.Q. Combinations of Tibetan tea and medicine food homology herbs: A new strategy for obesity prevention. *Food Sci. Nutr.* **2022**, *11*, 504-515.
70. Slattery, C.; Cotter, P.D.; O'Toole, P.W. Analysis of health benefits conferred by *Lactobacillus* species from Kefir. *Nutrients* **2019**, *11*, 1252.
71. Blackwood, B.P.; Yuan, C.Y.; Wood, D.R.; Nicolas, J.D.; Grothaus, J.S.; Hunter, C.J. Probiotic *Lactobacillus* species strengthen intestinal barrier function and tight junction integrity in experimental necrotizing enterocolitis. *J. Probiotics Health.* **2017**, *5*, 59-78.
72. Hu, X.; Guo, J.; Zhao, C.; Jiang, P.; Maimai, T.; Yanyi, L.; Cao, Y.; Fu, Y.; Zhang, N. The gut microbiota contributes to the development of Staphylococcus aureus-induced mastitis in mice. *ISME J.* **2020**, *14*, 1897-1910.
73. Quagliariello, A.; Del Chierico, F.; Russo, A.; Reddel, S.; Conte, G.; Lopetuso, L.R.; Ianiro, G.; Dallapiccola, B.; Cardona, F.; Gasbarrini, A.; et al. Gut microbiota profiling and gut-brain crosstalk in

children affected by pediatric acute-onset neuropsychiatric syndrome and pediatric autoimmune neuropsychiatric disorders associated with streptococcal infections. *Front. Microbiol.* **2018**, *9*, 675.
74. Dobrindt, U.; Hacker, J.H.; Svanborg, C. Preface. Between Pathogenicity and Commensalism. *Curr. Top. Microbiol. Immunol.* **2013**, *358*, v-vii.
75. Pilarczyk-Zurek, M.; Sitkiewicz, I.; Koziel, J. The clinical view on *Streptococcus anginosus* group-opportunistic pathogens coming out of hiding. *Front. Microbiol.* **2022**, *13*, 956677.
76. Waters, J.L.; Ley, R.E. The human gut bacteria Christensenellaceae are widespread, heritable, and associated with health. *BMC Biol.* **2019**, *17*, 83.
77. Mao, J.; Li; S.; Fu, R.; Wang, Y.; Meng, J.; Jin, Y.; Wu, T.; Zhang, M. Sea Cucumber Hydrolysate alleviates immunosuppression and gut microbiota imbalance induced by cyclophosphamide in Balb/c mice through the NF-κB pathway. *Foods* **2023**, *12*, 1604.
78. Dubois, M.; Gilles, K.A.; Hamilton, J.K.; Rebers, P.t.; Smith, F. Colorimetric method for determination of sugars and related substances. *Anal. Chem.* **1956**, *28*, 350-356.